Published in final edited form as:

Phys Chem Chem Phys. 2017 July 21; 19(27): 18036–18046. doi:10.1039/c7cp02849k.

Glucose Directs Amyloid-beta Into Membrane-Active Oligomers

Niraja Kedia[a], **Michael Almisry**[a], and **Jan Bieschke**[a,*]

[a]Department of Biomedical Engineering, Washington University in St. Louis, 63130 St. Louis, MO

Abstract

Oligomeric Amyloid-β 1–42 (Aβ-42) peptides are considered to be the most toxic species connected to the occurrence of Alzheimer's disease. However, not all aggregation conditions promote oligomer formation *in vitro*, raising the question whether oligomer formation *in vivo* also requires a specific suitable cellular environment. We recently found that interaction with neuronal membranes initiates aggregation of Aβ-42 and neuronal uptake. Our data suggest that small molecules in the extracellular space can facilitate the formation of membrane-active Aβ-42 oligomers. We analyzed the early stage of Aβ-42 aggregation in the presence of glucose and sucrose and found that these sugars strongly favor Aβ-42 oligomer formation. We characterized oligomers by dynamic light scattering, atomic force microscopy, immuno-transmission electron microscopy and fluorescence cross correlation spectroscopy. We found that Aβ-42 spontaneously and rapidly forms low molecular weight oligomers in the presence of sugars. Slightly acidic pH (6.7–7) greatly favors oligomer formation when compared to the extracellular physiological pH (7.4). Circular dichroism demonstrated that in presence of crowding agents Aβ-42 oligomers did not adopt a β-sheet structure. Unstructured oligomeric Aβ-42 interacted with membrane bilayers of giant unilamellar vesicles (GUV) and neuronal model cells, facilitated cellular uptake of Aβ-42, and inhibition of mitochondrial activity. Our data therefore suggest that elevated concentrations of glucose within the range observed in diabetic individuals (10 mM) facilitate the formation of membrane-active Aβ-42 oligomers.

Graphical Abstract

Amyloid-β-42 forms early unstructured oligomers at physiological glucose concentrations, which facilitates its cellular uptake and toxicity.

Introduction

Alzheimer's disease (AD) is the most common neurodegenerative disease. It is associated with the misfolding and aggregation of the 42 amino acid form of the Amyloid beta (Aβ-42) peptide and of the microtubule-associated protein tau [1–3]. While Aβ-42 accumulates in the brain in the form of fibrillar deposits, oligomeric species of Aβ-42 are strongly implicated in AD pathogenesis. Oligomers are assumed to be the cause of neuronal damage and their depletion may reduce neurotoxicity [4–7]. Aβ-42 and other amyloidogenic proteins can enter neurons via endocytic mechanisms [8–10]. We recently found that endocytic uptake of Aβ-42

*to whom correspondence should be addressed: bieschke@wustl.edu.

Electronic Supplementary Information (ESI) available: Supplementary figures. See DOI: 10.1039/x0xx00000x

and its aggregation are linked [11]. The uptake of monomeric Aβ-42 was preceded by aggregation of the peptide on the cellular membrane. This suggests that the Aβ-42 peptide interacts with the cellular membrane. Crowding of the peptide at the membrane surface may initiate amyloid formation [12].

Numerous studies have described the interaction of Aβ-42 peptides with lipid bilayers [13–17]. However, it is less clear which species of Aβ-42 – monomeric, oligomeric, protofibrillar, or fibrillar can interact with membrane bilayers with high affinity [18, 19]. Recent observations suggest that membrane binding of Aβ-42 may be linked to the formation of early oligomers [20, 21]. Experimental conditions in early studies of Aβ-42 membrane interaction also may have promoted oligomer formation [22–24].

Different types and sizes of Aβ-42 oligomers were identified *in vitro* [4, 25–27]. Aβ-42 oligomers compromise membrane integrity, which is a possible pathway of toxicity [23, 26, 28, 29]. However, in the nucleated polymerization mechanism of amyloid formation, oligomeric species are only metastable and are not strongly populated at low peptide concentrations [30, 31], raising the question which conditions promote the formation of Aβ-42 oligomers *in vitro* and *in vivo*. We investigated whether components of the extracellular medium, specifically glucose, promote formation of membrane active Aβ-42 species.

Type II diabetes and Alzheimer's disease are linked epidemiologically [32–34]. However, the mechanistic basis of this link is not yet clear [35]. Both diseases could be linked on the cellular, metabolic or molecular level. Specifically, elevated glucose levels might accelerate Aβ-42 oligomer formation. Osmolytes can alter protein folding pathways by burying hydrophobic residues and thus thermodynamically stabilizing the protein fold [36]. Trehalose and disaccharides alter Aβ-42 aggregation state and membrane permeabilization [37]. It should be noted that glucose and sucrose are often used in the formation of membrane model systems such as giant unilamellar vesicles (GUV), meaning that they may have played an undiscovered role in Aβ-42 membrane interaction.

Aggregation of Aβ-42 into β-sheet rich amyloid fibrils is a multistep process that proceeds through oligomeric and multimeric stages. Amyloidiphilic dyes such as Thioflavin T (ThT) are frequently used to measure the kinetics of amyloid cross-β sheet formation [38, 39]. However, ThT is blind to small unstructured oligomers [40]. Fluorescence based techniques, such as FlAsH labeling, fluorescence self-quenching, and single molecule fluorescence techniques have been powerful tools to quantify and characterize the formation of early unstructured Aβ-42 oligomers [40–46]. We probed if saccharides can directly alter the formation of early Aβ-42 oligomers and Aβ-42 membrane interaction. We characterized Aβ-42 oligomer formation in the presence of sucrose and glucose by dynamic light scattering (DLS), fluorescence cross correlation spectroscopy (FCCS) and immuno-transmission electron microscopy (TEM). We found that glucose at low millimolar concentrations promotes the formation of early, non-β-sheet oligomers of Aβ-42. Furthermore, oligomerization is most pronounced in a narrow range of pH between 6.7–7, which is lower than the pH of the extracellular space, but matches early endocytic vesicles. Aβ-42 oligomers transiently bind to the lipids of membrane bilayers. The same conditions

that promoted oligomer formation *in vitro* also promoted membrane binding, uptake and metabolic inhibition in neuronal model cells.

Materials and methods

Preparation of monomers of Aβ-42

Aβ-42 peptide (R. Volkmer, Charité, Berlin) was dissolved in hexafluoro-2-propanol and sonicated at room temperature for one hour in a water bath sonicator. After freezing in liquid nitrogen, HFIP was removed by lyophilization, and aliquots of the peptide were stored at −20 °C. To prepare unlabeled monomer, lyophilized Aβ-42 was dissolved in 10 mM NaOH, sonicated for 25 min in cold water bath, filtered through a 0.2 μm and a 30 kD membrane filter (Millipore). The monomers were then kept on ice before use. Aβ-42-Hilyte 488 (Aβ42–488) and Aβ-42-Hilyte 555 (Aβ42–555) labeled Aβ-42 and scrambled sequence Aβ-42 (Anaspec) was dissolved in 10mM NaOH and stored at −80°C. Scrambled Aβ was labeled with Alexa 488-NHS ester dye as described in [11]. Before use, labeled Aβ-42 was mixed with unlabeled Aβ-42 and then monomerized by membrane filtration as described above. In FCCS experiments without unlabeled Aβ-42, labeled Aβ-42 was dissolved in 3M guanidine hydrochloride (GdnHCl) for 10 minute and then diluted into assay buffer to a final GdnHCl concentration of 30 mM.

Preparation of Giant unilamellar vesicle (GUV)

DOPC (1,2-dioleoyl-sn-glycero-3-phosphocholine, Avanti Polar Lipids; 7.86 mg/ml) stock solution (10 μl) in chloroform was mixed with DiD dye (Invitrogen ;0.8 μl, 20 μM) and slowly dried onto two platinum wires, 1cm each. The two wires were inserted through the lid of a Teflon reaction vessel. The reaction vessel was filled with 230 μl 10% sucrose solutions and the container was placed in heating bath at −60°C. The wires were inserted into the liquid and a sinus wave AC current was applied at 10 Hz, 1.09–1.11 V for 2 hours. After two hours it was switched to 4 Hz, 1.3V for 30 minutes. The vesicles were then collected in a 0.6 ml Eppendorf tube and used within 2 days.

AFM sample preparation

10 μM freshly monomerised Aβ-42 was incubated in glucose (0, 5, 10 mM) in PBSN (K-phosphate 8 mM, pH 6.8; NaCl 150 mM) for 15 minutes. 10 μl aliquots of the above solutions were placed on a clean, freshly cleaved mica surface. After 10 minutes, the solvent was wicked off by filter paper and the mica was washed 4 times with 20 μl of water to remove salts and buffer from the sample. Images were obtained using tapping-mode AFM (Bruker).

Immuno-TEM grid preparation

Carbon films on 200-mesh copper grids (Ted Pella) were incubated with 5 μl of sample in the dark side of the grid for 10 minutes. The sample was wicked off from the grid and the grid was incubated with 10 μl 1% BSA in PBS to block any nonspecific binding. After that grids were incubated with anti Aβ antibody 6E10 (Signet), 1:100 diluted in PBS solution containing 0.1% BSA for 45 minutes. The grid was then washed by 7 drops of PBS buffer. After that grid was incubated with secondary anti mouse IgG antibody conjugated to 10 nm

diameter gold nanoparticles (Sigma Aldrich) diluted 1:20 in PBS buffer containing 0.1% BSA. 45 minutes later the grid was washed by 7 drops of PBS followed by 7 drops of water. Finally grids were stained by 2% Uranyl acetate solution for 2 minutes and air dried before collecting the images on a FEI Transmission Electron Microscope.

ThT Aggregation kinetics of Aβ-42

Freshly filtered monomeric Aβ-42 was dissolved in PBSN (K-phosphate 8 mM, pH 6.8; NaCl 150 mM) containing different concentration of glucose, or in GS buffer (solution of 190 mM glucose, 100 mM sucrose, 8 mM Potassium phosphate, pH 6.8) containing ThT dye (20 μM). Peptides were incubated at room temperature (25°C) or 37°C, with or without shaking for 5 second every 10 minutes, as indicated. The excitation and emission wavelengths were 420 and 480 nm respectively. The aggregation was monitored in Tecan infinite F200 plate reader in non-binding 96-well black wall, clear bottom (Corning 3651) plates.

Ultracentrifugation

Monomeric Aβ-42 (100 μl, 100 μM) or fibrillar Aβ-42 (100 μM monomer equivalent) that had been pre-incubated in PBSN buffer for 7 days, was incubated in PBSN + 9 mM glucose and 1 mM 6-NBDG. After incubation for 3 days at 4°C the solutions were centrifuged at 70,000 rpm (~200,000 × g) for 20 minutes at 4°C in a TL-100 centrifuge (Beckman). Supernatants were collected and pellets were washed with the same volume of PBSN + 10 mM glucose and centrifuged again. The pellet was dissolved in 100 μl of PBSN + 10 mM glucose. Fluorescence spectra of supernatant and pellet fractions were collected in a Spectramax i3× plate reader (Molecular Devices) in a 96 well plate with excitation at 474 nm at 25°C.

Dynamic light scattering (DLS)

Freshly filtered monomeric Aβ-42 was diluted into PBSN buffer (100 μl) with and without glucose (5 and 10 mM) in a disposable cuvette (Brand). Scatter intensities were measured in triplicate (10 traces of 10 s each) at 25°C, 173° backscatter measurement angle in a Malvern Zetasizer Nano ZS instrument with 633 nm laser excitation and a single-photon counting avalanche photodiode detector. All solutions were filtered through a 0.2 μm membrane filter prior to use. Calculation of correlation functions, cumulant analysis and size distribution analysis were performed using the Zetasizer software. The intensity-weighted mean diameter was derived from quadratic cumulant analysis. The polydispersity index of Aβ oligomers in glucose was below 0.4. Intensity-weighted size distributions were calculated by non-negative least squares (NNLS) analysis. Signals from samples without glucose were highly polydisperse and were not analyzed quantitatively.

Circular dichroism (CD)

Circular Dichroism (CD) was performed in a 1mm path length quartz cuvette in a Jasco J-810 spectropolarimeter. The scan speed was 50 nm / minute, data pitch of 0.5, response time 8 second, 5 continuous accumulations for the secondary structure of peptide. The scanning range was 190 to 260 nm. Molar ellipticities were calculated by subtracting the

ellipticity from the buffer control, and then multiplying by 10^6 and dividing by 41 and concentration of peptide used for the experiment. It should be noted that glucose and sucrose have significant positive ellipticities at wavelengths below 205 nm, so care was taken that signals stayed in the dynamic range of the CD spectrometer.

Fluorescence cross-correlation spectroscopy (FCCS)

FCCS was measured in a Confocor II (Zeiss) equipped with an Ar-ion laser (30 mW) as well as 543 nm (1 mW) and 633 nm (5 mW) He-Ne lasers. Samples were measured in 8 well lab-tek chambers that were previously coated with 0.1% BSA. Fluorescent Aβ-42 peptides were monomerized as described above. 5 sets of data each averaged over 30 seconds were collected with 488 nm (Aβ-42-Hilyte 488, Alexa 488) and 543 nm (Aβ-42-Hilyte 555) excitation at 50% laser power. In the green channel, the emission filter was a 505–530 nm bandpass while in the red channel a 585 nm long pass filter was used. Concentration of labeled Aβ-42 was in nanomolar range (10–50 nM). Diffusion data were fitted by one- or two-component models of three-dimensional diffusion at a fixed structural parameter $\kappa = 6$ in solution and with a two-dimensional free diffusion model on membranes. Autocorrelation data were fitted with triplet correction, cross correlation data without, as described in [47–49]. The following fitting models were used in the experiments.

3D single component diffusion:

$$G(\tau)=1+\frac{1}{N}\frac{1}{(1+\frac{\tau}{\tau_D})}\frac{1}{\sqrt{\left(1+\frac{\tau}{\tau_D\kappa^2}\right)}}$$

3D single component diffusion with triplet excitation

$$G(\tau)=1+(1+\frac{T}{1-T}e^{-\frac{\tau}{\tau_t}})\frac{1}{N}\frac{1}{(1+\frac{\tau}{\tau_D})}\frac{1}{\sqrt{\left(1+\frac{\tau}{\tau_D\kappa^2}\right)}}$$

3D - two component diffusion

$$G(\tau)=1+\frac{1}{N}\sum_{i=1,2}^{M}\frac{f_i}{(1+\frac{\tau}{\tau_{Di}})\sqrt{\left(1+\frac{\tau}{\tau_{Di}\kappa^2}\right)}}$$

Where, $\sum_{i=1,2}^{M} f_i=1$

N is number of particles, T is fraction of intersystem crossing, τ_D is diffusion time, τ_t is triplet correlation time, κ is structural parameter.

Z-scan FCS

Z-scan FCS was performed in the Confocor II. The excitation sources were 488 and 633 lasers. For the green channel (Aβ-42-Hilyte 488) a 505–530 nm band pass filter was used while in the red channel (DiD) a 650 nm long pass filter set was used. In order to monitor the membrane lipid diffusion, we stained GUV with DiD dye as described above. Aβ-42 diffusion was measured using Aβ-42-Hilyte 488. First, an immobile GUV was found by LSM imaging. Then the GUV of interest was positioned at the center of the laser focus, and a z-scan LSM image stack was recorded to confirm that the GUV was not moving. Then, cross- and autocorrelation curves were collected starting 4 μm above the GUV surface (bulk) at different position along the Z axis - at surface, inside as well as outside of GUV. The membrane surface was identified by the fastest diffusion time of the membrane lipid. The obtained autocorrelation curves were fitted by 2D one or two component diffusion with triplet excitation as indicated in the figures.

2D - two component diffusion with triplet excitation

$$G(\tau)=1+(1+\frac{T}{1-T}e^{-\frac{\tau}{\tau_t}})\frac{1}{N}\left(\frac{A}{(1+\frac{\tau}{\tau_{D1}})}+\frac{1-A}{\left(1+\frac{\tau}{\tau_{D2}}\right)}\right)$$

Calculation of oligomer sizes

Translational diffusion coefficients (D) of the biomolecules were calculated from diffusion times (τ_d):

$$\tau_d=\frac{r_0^2}{4D}$$

where, r_0 is the laser beam radius, D is the diffusion co-efficient and τ_D is the diffusion time. To calculate r_0 a dye with a known diffusion coefficient (Alexa 488) was used. Hydrodynamic radii were calculated using the Stokes-Einstein equation:

$$R_h=\frac{k_BT}{6\pi n_0 D}$$

where, R_h is the hydrodynamic radius, k_B is the Boltzmann constant, T is the temperature, n_0 is the viscosity and D is the diffusion co-efficient of the molecule.

MTT (3–(4,5–dimethylthiazol–2–yl)–2,5–diphenyltetrazolium bromide) assay

SH–EP cells were seeded into 96–well plates (7 k / well), grown to 80% confluency and treated with Aβ-42 that had been incubated at 5 μM concentration in PBSN for 2h or 24 h with and without 10 mM glucose. Aβ-42 was added to cells at the indicated concentrations and incubated for 3 days. MTT (1 mg / ml, 10 μl / well) was added and cells were incubated at 37 °C for 4 h. After that solubilization solution (10% Triton X-100, 0.1M HCl in

isopropanol, 100 μl / well) was added and incubated for overnight. The absorbance of MTT was recorded at 570 nm in a Tecan infinite F200 plate reader.

Aβ-42 uptake into SH-EP cell

Cells were seeded into a 8 well Lab-Tek chamber and grown to 80% confluency. Monomeric Aβ-42 (5 μM) was mixed with 0.2 % monomeric Aβ42–488 in PBSN buffer (0, 5, 10 mM glucose) for 30 minutes. The formed oligomeric Aβ-42 was diluted to 150 nM in CDMEM media and added to the cells. After 24 h incubation, the treated cells were washed twice with PBS and fixed with 4 % paraformaldehyde for 15 min at RT. 20 images of cells were collected by fluorescence microscopy (488 nm excitation) for each condition. The intensity of Aβ inclusions was evaluated in Image J analysis software. The total intensity of Aβ42–488 fluorescence was measured for each image and the average background fluorescence per pixel was subtracted. Plotted is a box plot of corrected fluorescence from 20 images per sample. P value was calculated from a two-tailed t-test assuming equal variances.

Silver staining of SDS PAGE gel

Required amount of sample were mixed with loading buffer and boiled at 95°C for 10 minutes. Then run the gel and after completion, the gel was silver stained by using silver staining kit (Sigma Aldrich) according to their provided protocol.

Results

Aβ-42 forms small, unstructured oligomers in the presence of sucrose and glucose

We tested the influence of glucose on Aβ-42 aggregation kinetics through dynamic light scattering and Thioflavin T (ThT) fluorescence (Fig. 1A, B). Freshly monomerized Aβ-42 (5 μM) was incubated in the presence of glucose (0, 5, 10 mM) in PBSN (K-phosphate 8 mM, pH 6.8; NaCl 150 mM). While ThT fluorescence revealed no influence of glucose on aggregation kinetics (Fig. 1B, Suppl. Fig. S1A, B), DLS revealed that Aβ-42 had formed aggregates prior to ThT binding (Fig. 1A). Glucose, at physiological concentration (5 mM) and at 10 mM concentration strongly accelerated the formation of Aβ-42 aggregates (Fig. 1A). When analyzing the hydrodynamic radii of aggregates, we found that in buffer without glucose, after 100 minutes the peptide formed large aggregates that were heterogeneous in size. In contrast, we found fairly homogenous aggregate populations of Aβ-42 in 10 mM glucose (Suppl Fig S2A). The size of these aggregates increased with time (Suppl. Fig. S2B.

We visualized Aβ-42 species by AFM under the same experimental conditions (Fig. 1C). Initially, after 15 min incubation, AFM revealed spherical oligomers of 4 ± 1 nm height (Fig. 1C). Oligomers of similar size were much more abundant in 10 mM glucose than in the absence of glucose. In a corresponding experiment, we visualized Aβ-42 structures after 30 min incubation by TEM and immuno-gold staining using anti-Aβ-42 antibody 6E10 in a buffer with physiological osmolarity. This buffer matched conditions in many membrane binding experiments (GS buffer, 190 mM glucose, 100 mM sucrose, 8 mM K phosphate, pH 6.8; Fig 1D). After 30 min, Aβ-42 had formed both small oligomer with diameters of few nanometers and larger oligomer structures with an average diameter of 100 ± 50 nm. Initial glucose-induced Aβ-42 oligomers remained soluble when analyzed by centrifugation at

200,000 × g and SDS-PAGE (Suppl. Fig. S3). These structures transitioned into amyloid fibrils after prolonged incubation (Fig. 1D). These data indicate that glucose and sucrose accelerate the formation of early Aβ-42 oligomers. Interestingly, glucose increased the fraction of SDS-stable Aβ-42 trimers in SDS-PAGE (Suppl. Fig. S3). In previous studies, such trimers correlated to Aβ-42 toxicity [4].

We investigated whether Aβ-42 adopted a β-sheet structure in the early oligomers using circular dichroism (CD) spectroscopy. Aβ-42 is unstructured as a monomer but adopts a β-sheet structure in amyloid fibrils[50]. The minimum at 200 nm, characteristic of unstructured polypeptides, was reduced over the course of 60 min incubation, both in the presence and absence of glucose / sucrose, indicating minor structural change (Fig. 2A, B). However, no β-sheet structures, indicated by a minimum at 218 nm, were formed. Therefore, we conclude that glucose-induced oligomers do not possess the cross-β motif that is characteristic for amyloid structures. Correspondingly, these structures were invisible in ThT aggregation assays since ThT did not bind to Aβ-42 during this phase of aggregation (Fig. 1B).

We then probed whether these early Aβ-42 oligomers bind glucose. To do so, we incubated monomeric Aβ-42 (100 μM) with a mixture of the fluorescent glucose analog 6-(N-(7-Nitrobenz-2-oxa-1,3-diazol-4-yl)amino)-6-Deoxyglucose (6-NBDG, 1 mM) and unlabeled glucose (9 mM) in PBSN. The recruitment of 6-NBDG into the pellet was evaluated after 3 day incubation at 4˚C by ultracentrifugation (200,000 × g). 6-NBDG fluorescence was measured in the supernatant and the pellet fractions (Fig. 2C, D). We found that 9% of 6-NBDG had co-precipitated with Aβ-42 oligomers. In contrast, only residual signals of 6-NBDG were detected in the pellet fraction when incubated with preformed fibrils (2.4%) under the same conditions (Fig. 2D) or in the absence of Aβ-42 (0.2%, Fig. 2D). This indicates that glucose binds specifically to early Aβ-42 oligomers with higher affinity than to preformed Aβ-42 fibrils.

Glucose can form Schiff base adducts to primary amines, such as lysine side chains, which can lead to covalent crosslinking of proteins by advanced glycation end products (AGE) [51, 52]. We tested for covalent adducts of glucose (10 mM in PBSN) to Aβ-42 (5 μM) by MALDI mass spectrometry under the same reaction conditions as above. However, we only observed masses corresponding to unmodified Aβ-42 mono-, di-, and trimers (Suppl. Fig. S4A–F). Likewise, analysis of Aβ-42 by SDS-PAGE did not reveal any covalent crosslinking of peptides (Suppl. Fig. S5). Therefore we conclude that sugar induced Aβ-42 oligomers without covalently modifying the Aβ-42 peptide. However, since higher-order oligomers could not be observed by MALDI, we cannot exclude the possibility that Aβ-42 forms Schiff base adducts in these structures.

Oligomer formation at nanomolar Aβ-42 concentrations

We utilized the sensitivity of FCCS in order to monitor early oligomer formation at micromolar and nanomolar concentrations. We monomerized a fluorescently labeled Aβ42–488 (16 nM) and Aβ42–555 (16 nM) by GdnHCl treatment. Monomeric Aβ-42 was then incubated in GS buffer for 60 minutes and auto- and cross-correlation curves were recorded at different time points (Fig. 3A, B). Cross-correlation amplitudes rapidly increased indicating the aggregation of Aβ-42 peptides. A plot of normalized cross-correlation

amplitudes (N_G/N_{RG}, Fig. 3C) vs. time shows that the fraction of Aβ-42 incorporated into oligomers increased with time [47–49]. At the same time autocorrelation signals indicated a decrease in the number of monomeric Aβ-42 molecules as monomers were incorporated into aggregates (Fig. 3B). Analysis of the diffusion times of the cross-correlation signal revealed rapid formation of small oligomers (τ_D = 100 ± 7 μs) corresponding to a hydrodynamic radius of ~2 nm (Fig. 3D). Similar results were obtained when co-incubating fluorescently labeled Aβ-42 (Aβ42–488, 18 nM; Aβ42–555, 25 nM) with unlabeled Aβ-42 (5 μM, Fig. 3E–H). Here, peptides were monomerized via membrane filtration at pH 10.5, similar to the experiments shown in Figs. 1 and 2. However, at micromolar peptide concentrations, larger aggregates were detected at incubation times > 30 min (denoted by * in Fig. 3H), corresponding to amorphous aggregates visualized by TEM. These aggregates could not be adequately be characterized by FCCS. This is most likely due to the inherent bias of diffusion-based FCS against relatively rare, large, and slow-moving aggregates [53, 54]. In contrast to the previous experiment, only weak increase in cross-correlation was observed in the absence of sugar (Suppl. Fig. S6A, B). No increase in cross-correlation signal was observed when mixing Aβ42–555 with scrambled sequence Aβ42–488 or when mixing dyes without Aβ (Suppl. Fig. S6C, D). This indicates that the observed cross-correlation signal corresponded to specific oligomer formation.

pH Dependence of glucose-induced oligomer formation

The extracellular space (pH 7.2–7.4), the cytosol (pH 7.0–7.4) and the endocytotic compartments (pH 6.0–6.5) offer environments of slightly different acidity [55], which could affect Aβ-42 oligomer formation. To test this hypothesis, we measured Aβ-42 oligomerization in the presence of glucose and sucrose as a function of pH and incubation time in the osmolyte buffer (Fig. 4) by FCCS spectroscopy as described in the previous section. We found a striking change of the normalized cross-correlation signal within a narrow pH range (Fig. 4), indicating that the formation of Aβ-42 oligomers is highly dependent on the local pH. We observed maximal oligomer formation at the range of pH 6.7–6.9, which corresponds to the pH found in early endocytic vesicles [55, 56]. This result suggests that budding endocytic vesicles on the membrane surface may be the ideal environment for Aβ-42 oligomer formation. These oligomers could bind to the membrane and aggregate into larger amyloid structures.

Aβ-42 oligomers transiently interact with membrane bilayers

Our next goal was therefore to investigate the binding of Aβ-42 oligomers to membrane bilayers. We used giant unilamellar vesicles (GUV) as a membrane model system for single molecule binding experiments [57, 58]. GUVs of DOPC, labeled with the membrane dye DiD, were generated by electro-formation, carefully diluted into GS buffer and settled on a glass coverslip (Fig. 5). When adding Aβ-42 (5 μM + Aβ42–555, 50 nM), we found no strong enrichment of fluorescently labeled Aβ-42 on the GUV membrane (Suppl Fig. S7), suggesting that Aβ-42 might transiently interact with the membrane bilayer. Therefore, we took the advantage of Z-scan fluorescence correlation spectroscopy (Z-scan FCS), to characterize the membrane interaction of Aβ-42 [59, 60].

We placed the FCS volume 4 μm above the GUV, added Aβ-42 (5 μM + Aβ42–488, 50 nM) and moved the focal volume down by steps of 0.2 nm. We used the autocorrelation signal of the DiD dye to pinpoint the position of the membrane, which is the z-position at which the diffusion time of the membrane marker is minimal and its correlation amplitude is maximal (Fig. 5) [59, 60]. While performing FCS measurements, we confirmed by repeated confocal imaging that the GUV under study was not moving. Fig. 5 shows representative correlation curves of Aβ42–488 (left) and DiD (right) recorded above the GUV membrane and on the membrane surface.

Figures 6A, B, and C show plots of autocorrelation amplitudes, counts per molecule (cpm), and diffusion times of the red and the green fluorescence channel as functions of z-position, respectively. Maxima of correlation amplitudes and cpm of the membrane dye combined with minima of the diffusion time indicated the membrane position at 246.5 ± 0.2 nm. Since Aβ42–488 was present both in the bulk solution and on the membrane, its diffusion time increased as the focus was moved into the membrane bilayer, while the count rate per molecule dropped to an intermediate level. On the membrane, the average number of Aβ42–488 molecules in the detection volume increased ten-fold from 30 to 300 and then dropped to 0, since no Aβ-42 molecules were present inside the GUV (Fig. 6B). At the same time the average diffusion time of Aβ-42 increased from 90 ± 5 μs to 370 ± 200 μs (Fig. 6C), indicating that Aβ-42 on the membrane diffused much more slowly than in solution. In contrast cpm of the Aβ-42 channel increased only moderately by 40% on the membrane when compared to the bulk solution, suggesting that Aβ-42 species in solution and on the membrane had similar brightness and therefore contained similar numbers of monomers.

When comparing the membrane dye DiD (1230 ± 110 μs) and Aβ-42 (370 ± 220 μs ; Fig. 6C) diffusion times corresponded to diffusion constants of 11 $\mu m^2 s^{-1}$ and 28 $\mu m^2 s^{-1}$ respectively[61] on the membrane. We noted that, even though Aβ-42 diffused much more slowly on the membrane than in solution, its diffusion time was faster than that of the membrane dye. A faster diffusion of Aβ-42 than the lipid dye suggests that Aβ-42 oligomers were not incorporated into the membrane but only bound transiently and moved by a ‘hopping’ mechanism [62].

Glucose induced Aβ oligomers accumulate on neuronal cell membranes

Our *in vitro* data suggest that glucose facilitate the formation of membrane-active Aβ-42 species, and may thus accelerate Aβ-42 binding to cellular membranes and its uptake into neurons. We tested whether glucose induced oligomers could accumulate on the surfaces of cell membranes of neuronal model cells. We incubated Aβ-42 (5 μM + Aβ42–488, 8 nM) for 30 min in PBSN (0, 5, 10 mM glucose) and then diluted the Aβ-42 to 150 nM into the medium of human neuroblastoma (SH-EP) cells, so that the cells do not experience differences in osmolarity in the experiments. At this concentration, SH-EP cells do not internalize monomeric Aβ-42 [11]. After 24 h, we imaged cells by fluorescence microscopy and quantified cellular Aβ-42 inclusions via Aβ42–488 fluorescence intensity (Fig. 7A). The amount of Aβ-42 found in inclusions correlated with glucose concentration during incubation. Glucose-induced Aβ-42 oligomers formed significantly more inclusions than Aβ-42 incubated in the absence of glucose (Fig. 7A). These inclusions were partially

associated with the cell membrane and partially internalized into the cell. This indicates that glucose-induced Aβ-42 oligomers are indeed membrane-active and bind to cellular membranes. This furthermore suggests that elevated glucose levels facilitate the formation of membrane-active early oligomers and their uptake into neurons. However, we cannot exclude the possibility that the glucose that is bound to Aβ oligomers influences the cells directly.

Glucose induced Aβ oligomers inhibit mitochondrial activity

Accumulation and uptake of Aβ-42 into neurons are correlated with mitochondrial inhibition[11]. This suggests that the induction of membrane active oligomers by glucose could be a first step in Aβ-42 toxicity. We tested whether Aβ-42 oligomers formed in buffers with elevated glucose concentration could inhibit mitochondrial metabolism of human neuroblastoma (SH-EP) cells by measuring their capacity to reduce the dye 3-(4,5-dimethylthiazol-2-yl)-2,5-diphenyltetrazolium bromide (MTT, Fig. 7B)[7, 63]. Aβ-42 (5μM) was incubated in PBSN + 10 mM glucose for 2 h or 24 h and then added to the medium of SH-EP cells. Glucose induced oligomers inhibited MTT reduction significantly more than Aβ-42 incubated in PBSN without glucose. These data suggest that elevated glucose may accelerate the formation of toxic Aβ-42 oligomers.

Discussion

Aβ-42 oligomers have been identified as a main toxic species in AD [5]. Endocytic uptake and toxicity of Aβ-42 are tightly linked [8, 9, 11]. We found that aggregation of Aβ-42 is a prerequisite for its efficient uptake and that Aβ-42 aggregates in a compartment on the cell membrane if endocytosis is inhibited [11]. This raises the question if monomeric, oligomeric, or fibrillar forms of Aβ-42 initially interact with the membrane. This question is not yet resolved [18, 64]. Aβ-42 monomers can interact with membranes at high concentrations through electrostatic interactions [22, 23], however, monomeric Aβ-42 binds to neutral membrane bilayers with poor affinity, whereas oligomeric forms of Aβ-42 interact with lipid bilayers and bind to cell membranes [11, 18].

We found that Aβ-42 rapidly forms oligomers in the presence of glucose and sucrose at nanomolar peptide concentrations. These early oligomers did not bind to ThT and did not have β-sheet structure. Oligomer formation occurred at physiological glucose levels in the range observed in healthy to diabetic individuals (5 – 10 mM), which raises the possibility that oligomers may be the form of Aβ-42 that is present under physiological conditions. Alternatively, since glucose concentration in the ISF (interstitial fluid) is about twofold lower than in the serum [65], our results raise the possibility that Aβ-42 exists in equilibrium between monomers and oligomers that can be shifted towards oligomers in the case of hyperglycemia.

Thus, hyperglycemia may provide a mechanistic link between diabetes and Alzheimer's disease. Type 2 diabetes is strongly associated with an increased risk of AD and elevated glucose levels accelerate the progression of mild cognitive impairment towards dementia[34, 66, 67]. The link between glucose and Aβ-42 may be twofold: On one hand acute hyperglycemia in the blood serum increases both glucose levels in the ISF and Aβ-42

levels [65]. On the other hand, we find that hyperglycemia accelerates the formation of oligomeric species of Aβ-42 that may initiate the pathway towards amyloid formation.

How does glucose effect the oligomerization of Aβ-42? Glucose molecules co-precipitate with Aβ-42, if they are present during oligomerization, but not if they are added after mature Aβ-42 fibrils have already been formed (Fig. 2C and 2D). This implies that Aβ-42 oligomers incorporate glucose while Aβ-42 fibrils have a much lower affinity to glucose than monomeric or oligomeric Aβ-42. Studies of Aβ-42 amyloid formation in the 1990s have observed that extensive glycation of Aβ-42 and other amyloidogenic peptides alters their aggregation propensity and may stabilize seeding competent fibrils [6869]. This effect was attributed to advanced glycation end products (AGE) that covalently modify and crosslink Aβ-42 molecules. AGE have been implicated in aging and age-related diseases, and specifically in AD and diabetes [7052]. AGE form via Maillard reaction at neutral pH in the presence of phosphate [52]. Modification proceeds via initial Schiff base formation with primary amines, such as lysines, followed by structural rearrangement into Amadori products [52, 71]. Subsequent oxidation and condensation into AGE can be catalyzed by transition metal ions [51]. While quantitative formation of AGE usually requires incubation with molar concentration of glucose at neutral pH for several months, the initial modification of Aβ-42 by Schiff base formation with glucose was observed within 24 h or less [51]. However, our data give no evidence that AGE are formed during early Aβ-42 aggregation. Rather, they suggest that glycation could exacerbate Aβ-42 toxicity by different, previously uncharacterized mechanism, i.e. the induction of membrane-active Aβ-42 oligomers.

Conclusions

Our data suggest that elevated concentrations of glucose within the range observed in diabetic individuals (10 mM) initiate the formation of mostly disordered, but membrane-active Aβ-42 oligomers. These oligomers can enter neuronal model cells and inhibit mitochondrial activity. Therefore our results suggest that elevated glucose levels can exacerbate an early step in Aβ-42 aggregation and toxicity. This effect may link type 2 diabetes and Alzheimer's disease on a molecular level.

Supplementary Material

Refer to Web version on PubMed Central for supplementary material.

Acknowledgments

This research was financially supported by the DRC at Washington University (NIH Grant No. 5 P30 DK020579), and the German Science Foundation (DFG, BI 1409/1-1). We gratefully acknowledge S. Singamaneni and E. Elson Washington University in St. Louis for the use of ConfoCor and AFM instrumentation, the Nano Research Facility, Washington University in St. Louis, and the NIH / NIGMS Biomedical Mass Spectrometry Resource at Washington University in St. Louis, MO, which is supported by National Institutes of Health \ National Institute of General Medical Sciences Grant # 8P41GM103422. We thank K. Garai and C. Frieden, Washington University in St. Louis for helpful discussions and for their help in GUV preparation.

References

1. Masters CL, Simms G, Weinman NA, Multhaup G, McDonald BL, Beyreuther K. Proceedings of the National Academy of Sciences of the United States of America. 1985; 82:4245–4249. [PubMed: 3159021]
2. Masters CL, Beyreuther K. Brain pathology. 1991; 1:226–227. [PubMed: 1669713]
3. Yanamandra K, Kfoury N, Jiang H, Mahan TE, Ma S, Maloney SE, Wozniak DF, Diamond MI, Holtzman DM. Neuron. 2013; doi: 10.1016/j.neuron.2013.07.046
4. Walsh DM, Klyubin I, Fadeeva JV, Cullen WK, Anwyl R, Wolfe MS, Rowan MJ, Selkoe DJ. Nature. 2002; 416:535–539. [PubMed: 11932745]
5. Haass C, Selkoe DJ. Nature reviews Molecular cell biology. 2007; 8:101–112. [PubMed: 17245412]
6. Bieschke J, Herbst M, Wiglenda T, Friedrich RP, Boeddrich A, Schiele F, Kleckers D, Lopez del Amo JM, Gruning BA, Wang Q, Schmidt MR, Lurz R, Anwyl R, Schnoegl S, Fandrich M, Frank RF, Reif B, Gunther S, Walsh DM, Wanker EE. Nature chemical biology. 2012; 8:93–101.
7. Cohen E, Bieschke J, Perciavalle RM, Kelly JW, Dillin A. Science. 2006; 313:1604–1610. [PubMed: 16902091]
8. Friedrich RP, Tepper K, Ronicke R, Soom M, Westermann M, Reymann K, Kaether C, Fandrich M. Proceedings of the National Academy of Sciences of the United States of America. 2010; 107:1942–1947. [PubMed: 20133839]
9. Hu X, Crick SL, Bu G, Frieden C, Pappu RV, Lee JM. Proceedings of the National Academy of Sciences of the United States of America. 2009; 106:20324–20329. [PubMed: 19910533]
10. Mirbaha H, Holmes BB, Sanders DW, Bieschke J, Diamond MI. The Journal of biological chemistry. 2015; 290:14893–14903. [PubMed: 25887395]
11. Jin S, Kedia N, Illes-Toth E, Haralampiev I, Prisner S, Herrmann A, Wanker EE, Bieschke J. The Journal of biological chemistry. 2016; 291:19590–19606. [PubMed: 27458018]
12. Yeung PS, Axelsen PH. Journal of the American Chemical Society. 2012; 134:6061–6063. [PubMed: 22448820]
13. McLaurin J, Chakrabartty A. The Journal of biological chemistry. 1996; 271:26482–26489. [PubMed: 8900116]
14. Chauhan A, Ray I, Chauhan VP. Neurochemical research. 2000; 25:423–429. [PubMed: 10761989]
15. Curtain CC, Ali FE, Smith DG, Bush AI, Masters CL, Barnham KJ. The Journal of biological chemistry. 2003; 278:2977–2982. [PubMed: 12435742]
16. Matsuzaki K. Biochimica et biophysica acta. 2007; 1768:1935–1942. [PubMed: 17382287]
17. Small DH, Maksel D, Kerr ML, Ng J, Hou X, Chu C, Mehrani H, Unabia S, Azari MF, Loiacono R, Aguilar MI, Chebib M. Journal of neurochemistry. 2007; 101:1527–1538. [PubMed: 17286584]
18. Nag S, Chen J, Irudayaraj J, Maiti S. Biophysical journal. 2010; 99:1969–1975. [PubMed: 20858443]
19. Bateman DA, Chakrabartty A. Biophysical journal. 2009; 96:4260–4267. [PubMed: 19450496]
20. Nag S, Sarkar B, Chandrakesan M, Abhyanakar R, Bhowmik D, Kombrabail M, Dandekar S, Lerner E, Haas E, Maiti S. Physical chemistry chemical physics : PCCP. 2013; 15:19129–19133. [PubMed: 24121316]
21. Sarkar B, Das AK, Maiti S. Frontiers in physiology. 2013; 4:84. [PubMed: 23781202]
22. Terzi E, Holzemann G, Seelig J. Biochemistry. 1997; 36:14845–14852. [PubMed: 9398206]
23. Hertel C, Terzi E, Hauser N, Jakob-Rotne R, Seelig J, Kemp JA. Proceedings of the National Academy of Sciences of the United States of America. 1997; 94:9412–9416. [PubMed: 9256496]
24. Kremer JJ, Pallitto MM, Sklansky DJ, Murphy RM. Biochemistry. 2000; 39:10309–10318. [PubMed: 10956020]
25. McLean CA, Cherny RA, Fraser FW, Fuller SJ, Smith MJ, Beyreuther K, Bush AI, Masters CL. Annals of neurology. 1999; 46:860–866. [PubMed: 10589538]
26. Lashuel HA, Hartley D, Petre BM, Walz T, Lansbury PT Jr. Nature. 2002; 418:291.
27. Kayed R, Head E, Thompson JL, McIntire TM, Milton SC, Cotman CW, Glabe CG. Science. 2003; 300:486–489. [PubMed: 12702875]

28. Widenbrant MJ, Rajadas J, Sutardja C, Fuller GG. Biophysical journal. 2006; 91:4071–4080. [PubMed: 17098805]
29. Sciacca MF, Kotler SA, Brender JR, Chen J, Lee DK, Ramamoorthy A. Biophysical journal. 2012; 103:702–710. [PubMed: 22947931]
30. Powers ET, Powers DL. Biophysical journal. 2006; 91:122–132. [PubMed: 16603497]
31. Powers ET, Powers DL. Biophysical journal. 2008; 94:379–391. [PubMed: 17890392]
32. Huang CC, Chung CM, Leu HB, Lin LY, Chiu CC, Hsu CY, Chiang CH, Huang PH, Chen TJ, Lin SJ, Chen JW, Chan WL. PloS one. 2014; 9:e87095. [PubMed: 24489845]
33. Haan MN. Nature clinical practice Neurology. 2006; 2:159–166.
34. Ott A, Stolk RP, van Harskamp F, Pols HA, Hofman A, Breteler MM. Neurology. 1999; 53:1937–1942. [PubMed: 10599761]
35. Akter K, Lanza EA, Martin SA, Myronyuk N, Rua M, Raffa RB. British journal of clinical pharmacology. 2011; 71:365–376. [PubMed: 21284695]
36. Kumar R. Archives of biochemistry and biophysics. 2009; 491:1–6. [PubMed: 19769937]
37. Qi W, Zhang A, Good TA, Fernandez EJ. Biochemistry. 2009; 48:8908–8919. [PubMed: 19637920]
38. LeVine H 3rd. Methods in enzymology. 1999; 309:274–284. [PubMed: 10507030]
39. Bieschke J, Zhang Q, Powers ET, Lerner RA, Kelly JW. Biochemistry. 2005; 44:4977–4983. [PubMed: 15794636]
40. Lee J, Culyba EK, Powers ET, Kelly JW. Nature chemical biology. 2011; 7:602–609. [PubMed: 21804535]
41. Sengupta P, Garai K, Sahoo B, Shi Y, Callaway DJ, Maiti S. Biochemistry. 2003; 42:10506–10513. [PubMed: 12950178]
42. Garai K, Sureka R, Maiti S. Biophysical journal. 2007; 92:L55–57. [PubMed: 17237197]
43. Garai K, Frieden C. Proceedings of the National Academy of Sciences of the United States of America. 2013; 110:3321–3326. [PubMed: 23401512]
44. Tjernberg LO, Pramanik A, Bjorling S, Thyberg P, Thyberg J, Nordstedt C, Berndt KD, Terenius L, Rigler R. Chemistry & biology. 1999; 6:53–62. [PubMed: 9889152]
45. Drews A, Flint J, Shivji N, Jonsson P, Wirthensohn D, De Genst E, Vincke C, Muyldermans S, Dobson C, Klenerman D. Scientific reports. 2016; 6:31910. [PubMed: 27553885]
46. Dhavale DD, Tsai C, Bagchi DP, Engel LA, Sarezky J, Kotzbauer PT. The Journal of biological chemistry. 2017; doi: 10.1074/jbc.M116.767053
47. Bieschke, J., Schwille, P. Fluorescence Microscopy and Fluorescence Probes. Slavik, J., editor. Vol. 2. Springer; New York: 1998. p. 81-86.
48. Bacia K, Haustein E, Schwille P. Cold Spring Harbor protocols. 2014; 2014:709–725. [PubMed: 24987147]
49. Bacia K, Schwille P. Nature protocols. 2007; 2:2842–2856. [PubMed: 18007619]
50. Serpell LC. Biochimica et biophysica acta. 2000; 1502:16–30. [PubMed: 10899428]
51. Loske C, Gerdemann A, Schepl W, Wycislo M, Schinzel R, Palm D, Riederer P, Munch G. European journal of biochemistry / FEBS. 2000; 267:4171–4178.
52. Srikanth V, Maczurek A, Phan T, Steele M, Westcott B, Juskiw D, Munch G. Neurobiology of aging. 2011; 32:763–777. [PubMed: 19464758]
53. Giese A, Bieschke J, Eigen M, Kretzschmar HA. Archives of virology Supplementum. 2000:161–171. [PubMed: 11214919]
54. Bieschke J, Giese A, Schulz-Schaeffer W, Zerr I, Poser S, Eigen M, Kretzschmar H. Proceedings of the National Academy of Sciences of the United States of America. 2000; 97:5468–5473. [PubMed: 10805803]
55. Sorkin A, Von Zastrow M. Nature reviews Molecular cell biology. 2002; 3:600–614. [PubMed: 12154371]
56. Huotari J, Helenius A. The EMBO journal. 2011; 30:3481–3500. [PubMed: 21878991]
57. Korlach J, Schwille P, Webb WW, Feigenson GW. Proceedings of the National Academy of Sciences of the United States of America. 1999; 96:8461–8466. [PubMed: 10411897]

58. Bacia K, Schwille P. Methods. 2003; 29:74–85. [PubMed: 12543073]
59. Steinberger T, Machan R, Hof M. Methods in molecular biology. 2014; 1076:617–634. [PubMed: 24108647]
60. Stefl M, Kulakowska A, Hof M. Biophysical journal. 2009; 97:L01–03. [PubMed: 19651025]
61. Roden M. Wiener klinische Wochenschrift. 2016; 128(Suppl 2):S37–40. [PubMed: 27052219]
62. Metzler R, Jeon JH, Cherstvy AG. Biochimica et biophysica acta. 2016; 1858:2451–2467. [PubMed: 26826272]
63. Ehrnhoefer DE, Bieschke J, Boeddrich A, Herbst M, Masino L, Lurz R, Engemann S, Pastore A, Wanker EE. Nature structural & molecular biology. 2008; 15:558–566.
64. Nag S, Sarkar B, Bandyopadhyay A, Sahoo B, Sreenivasan VK, Kombrabail M, Muralidharan C, Maiti S. The Journal of biological chemistry. 2011; 286:13827–13833. [PubMed: 21349839]
65. Macauley SL, Stanley M, Caesar EE, Yamada SA, Raichle ME, Perez R, Mahan TE, Sutphen CL, Holtzman DM. The Journal of clinical investigation. 2015; 125:2463–2467. [PubMed: 25938784]
66. Crane PK, Walker R, Larson EB. N Engl J Med. 2013; 369:1863–1864.
67. Li W, Wang T, Xiao S. Neuropsychiatric disease and treatment. 2016; 12:2489–2495. [PubMed: 27729793]
68. Kapurniotu A, Bernhagen J, Greenfield N, Al-Abed Y, Teichberg S, Frank RW, Voelter W, Bucala R. European journal of biochemistry / FEBS. 1998; 251:208–216.
69. Vitek MP, Bhattacharya K, Glendening JM, Stopa E, Vlassara H, Bucala R, Manogue K, Cerami A. Proceedings of the National Academy of Sciences of the United States of America. 1994; 91:4766–4770. [PubMed: 8197133]
70. Monnier VM, Cerami A. Science. 1981; 211:491–493. [PubMed: 6779377]
71. Amadori M. Atti Reale Accad Nazl Lincei. 1929; 9:68–73.

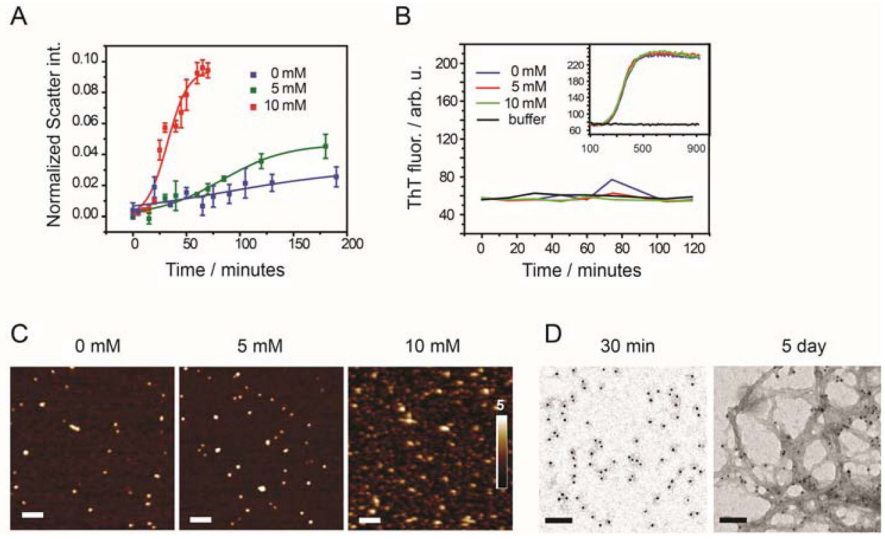

Figure 1.

(A) Scatter intensity of freshly prepared monomeric Aβ-42 (concentration 10 μM) incubated at 25°C in PBSN buffer with 0 mM glucose (blue), 5 mM glucose (green) and 10 mM glucose (red) at pH 6.8 obtained from dynamic light scattering. Scatter signals of buffer without Aβ was subtracted and intensities were normalized to toluene scatter signals; means ± SD, n = 3. (B) ThT fluorescence of 10 μM freshly filtered Aβ-42 allowed to aggregate in the DLS cuvette under the same conditions as in (A). Samples were collected at different time point, diluted 3-fold into same buffer + ThT (20μM). Within 2 hours of incubation no ThT positive signal was found. After 2 h the diluted sample was further incubated at 37˚C (inset) and ThT-positive aggregates were formed. (C) AFM images of 10 μM freshly filtered Aβ-42 incubated for 15 minutes in PBSN buffer containing 0 mM, 5 mM, and 10 mM glucose at pH 6.8. Scale bars 100 nm. (D) Immuno TEM images of 5 μM Aβ-42 incubated in GS buffer of pH 6.8 after 30 minutes and after 5 day incubation; Scale bars 100 nm.

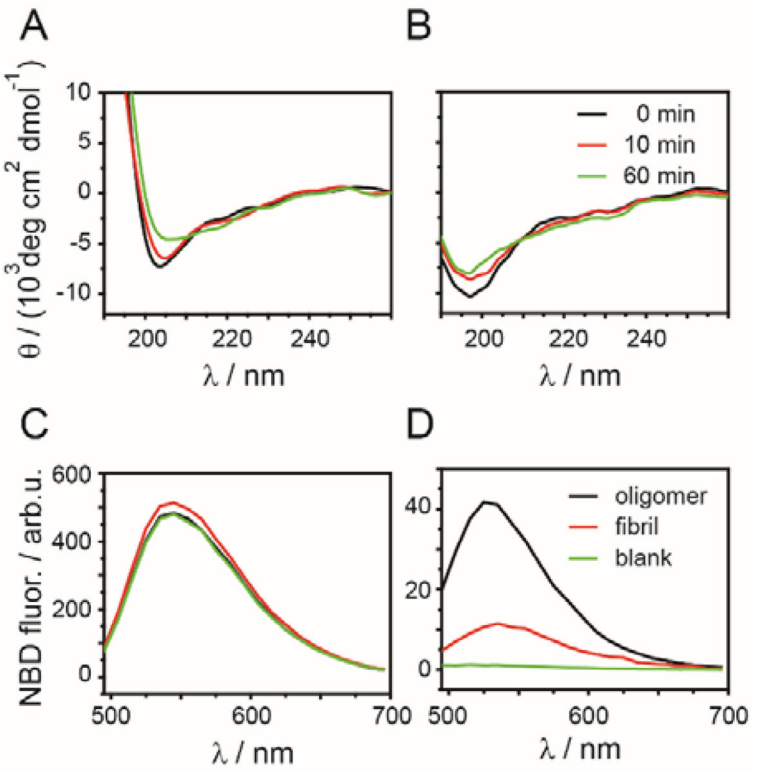

Figure 2.

(A) Circular dichroism (CD) spectra of 5 μM freshly filtered Aβ-42 (A) in GS buffer (190 mM glucose, 100 mM sucrose, 8 mM K-phosphate, pH 6.8) and (B) in K-phosphate buffer, pH 6.8 at different incubation times (0, 10, and 60 min). Fluorescence spectra of 6-NBDG measured in the supernatant (C) and in the washed pellet (D) of 100 μM Aβ-42 oligomer, preformed fibrils and buffer control (blank).

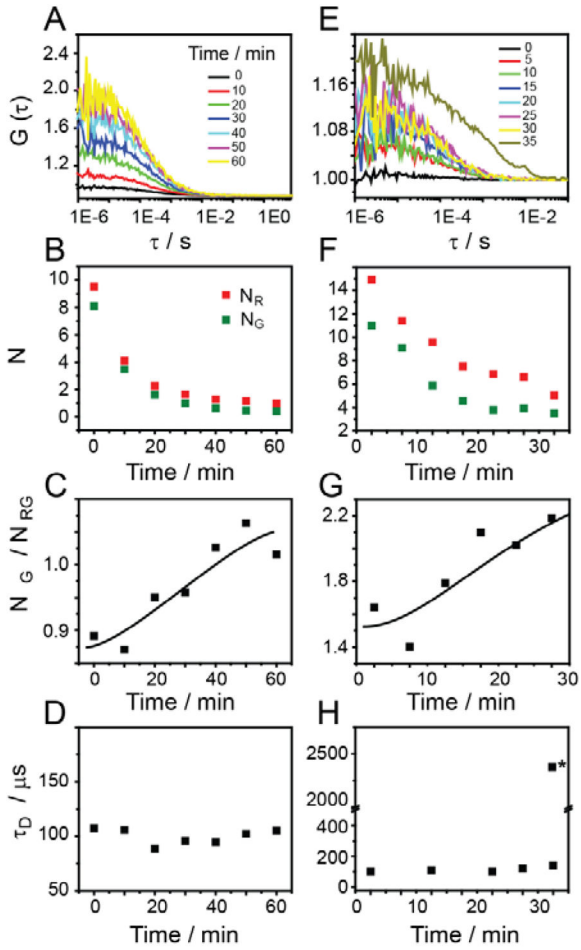

Figure 3.

(A) Fluorescence cross correlation signals of monomeric Aβ42-hilyte 488 and Aβ42-hilyte 555 at 16 nM concentration in GS buffer. The cross-correlation amplitude gradually increased over time due to oligomer formation. Plots of (B) total particle numbers in green channel and red channel, (C) relative cross-correlation amplitude N_G/N_{RG}, and (D) diffusion time (τ_D) vs incubation time for Aβ42–488 and Aβ42–555 in GS buffer (E) Cross-correlation curve of Aβ42–488 and Aβ42–555 mixed with 5 μM Aβ-42 in GS buffer. (F) (G) and (H) particle number, N_G/N_{RG}, and diffusion time is plotted against time for Aβ42–488 and Aβ42–555 in GS buffer with 5 μM Aβ-42. All correlation curves were fitted by a single component 3D model, except *, which denotes large aggregate component derived from a two-component fit at t = 35 min. All other correlation curves were best fitted by a single diffusing component.

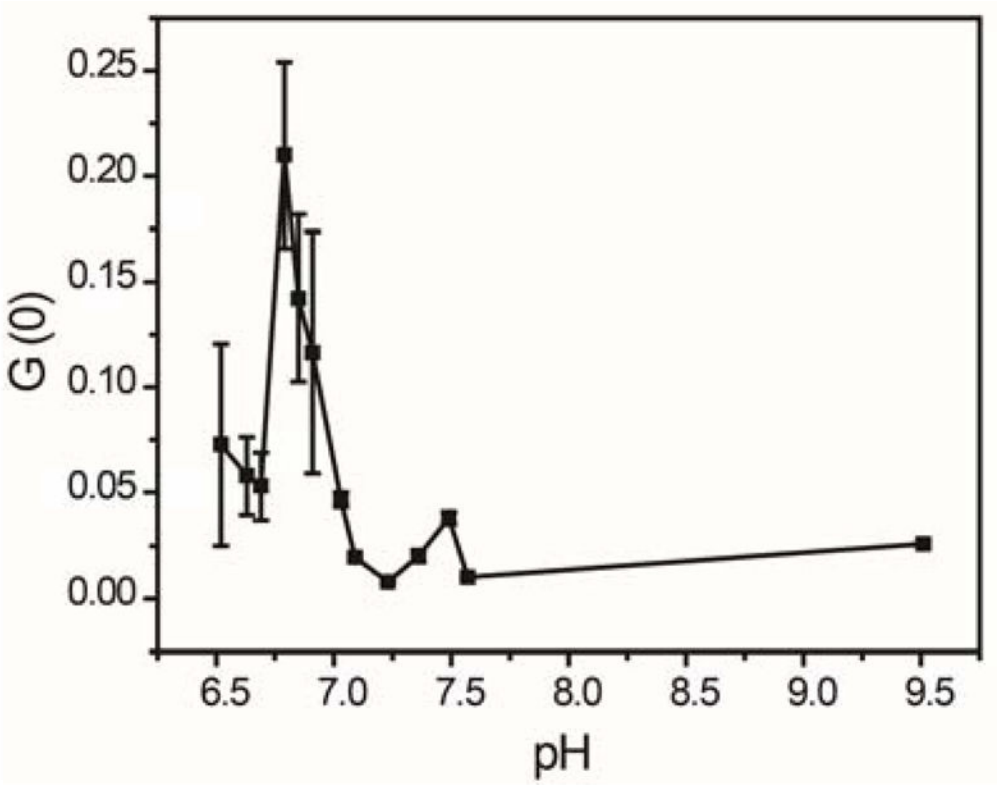

Figure 4.

Fluorescence cross correlation was measured for 5 μM freshly filtered monomeric Aβ-42 with 90 nM concentration of Aβ42–488 and Aβ42–555 in GS buffer of different pH. A plot of G(0) vs pH after 60 minute incubation shows that in the pH range 6.8–7.0, Aβ-42 forms the maximum number of oligomers. The graph show means ± SD of cross correlation amplitudes from quintuplicate measurements.

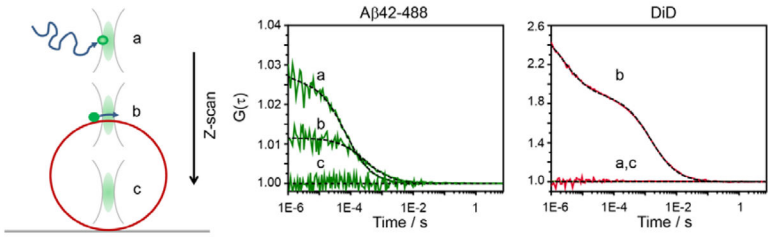

Figure 5.

Schematic representation of Z-scan FCS performed in DiD labeled GUV in GS buffer containing 5 μM Aβ-42 along with 50 nM concentration of monomeric Aβ42–488. The focal volume was moved from above the GUV surface (a) to the surface (b) to the inside an immobilised GUV (c). Autocorrelation curve above, near the surface and inside of an immobilised GUV, for Aβ42–488 and DiD dye, respectively are shown. Dashed lines represent fits for 2D diffusion with a single component and triplet excitation.

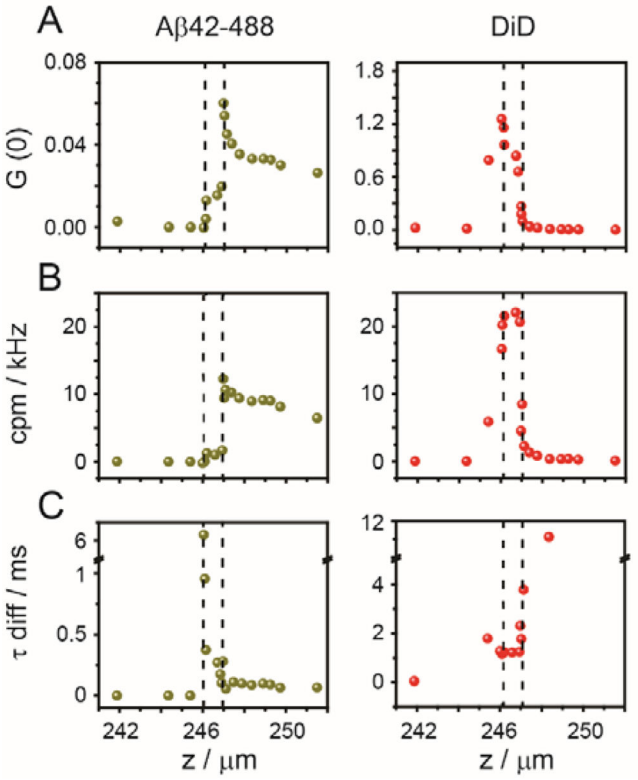

Figure 6.

Z-scan FCS performed in DiD labeled GUV in GS buffer containing 5 μM Aβ-42 along with 50 nM concentration of monomeric Aβ42–488 and data were fitted as in Fig. 5. The plots show as a function of z-position: (A) G(0), (B) counts per molecule (cpm), and (C) diffusion time for Aβ42–488 and DiD dye. The region inside the dotted lines indicates data points near the surface of the GUV.

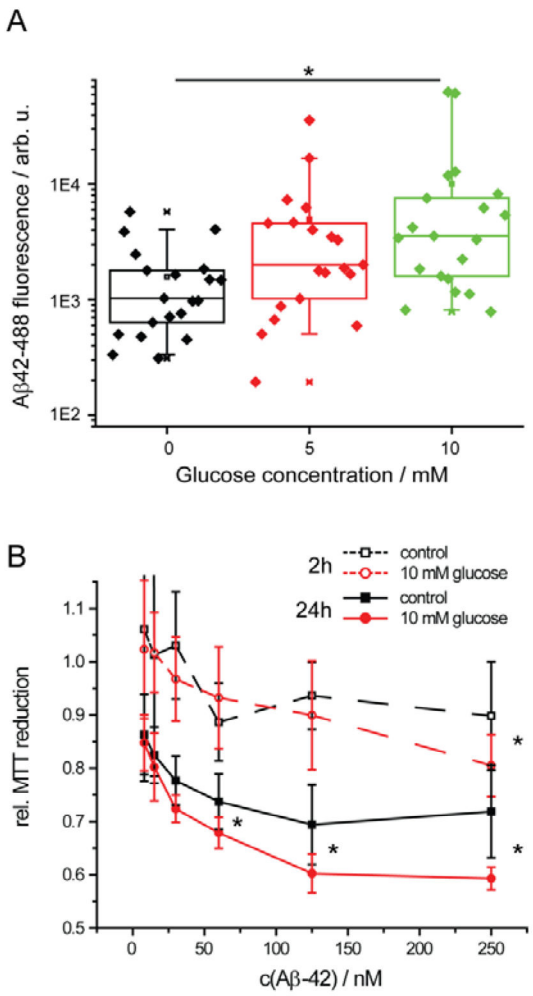

Figure 7.

(A) Intracellular Aβ42–488 fluorescence in SH-EP cells as a function of glucose concentration; n = 20. Here, n is the number of images. Each image contained 30–50 cells. (B) Mitochondrial activity of SH-EP cells after addition of Aβ-42. Aβ-42 (5 μM) was pre-incubated for 2h or 24h in PBSN +/− glucose and then added to the cell culture media for 3 d; n = 5, * $p < 0.05$. Incubation in the presence of glucose increased cellular uptake and mitochondrial inhibition by Aβ-42.